# Modeling Approach for An Aortic Dissection with Endovascular Stenting*

Yasuyuki Shiraishi, Tomoyuki Yambe, Andrew J. Narracott, Akihiro Yamada, *Member, IEEE*
Ryosuke Morita, Yi Qian, and Kazuhiko Hanzawa

*Abstract*— **Repair of dissected aorta requires remodeling the structure of the media. Modeling approaches specific to endovascular stenting for aortic dissection have been reported. We created a goat model of descending thoracic aortic dissection and reproduced its morphological characteristics in a mock circulatory system. The purpose of this study was to examine a newly developed aortic stent which was capable of installing to the aortic dissected lesion for biomedical hemodynamics point of view. In this study, we examined the changes in hemodynamics of dissected lesions and the amelioration by endovascular stent intervention. Firstly, we performed animal experiments with the dissected aorta and examined the effects of stenting on volumetric changes in the false lumen. Secondly, we made several types of 3-D stereolithographic dissected aortic models with silicone rubber membrane between the false and the true lumens. Then, the hemodynamic characteristics in each model were evaluated in the pulsatile flow conditions in a mock circulatory system. These modelling approaches enabled the quantitative examination of post-therapeutic effects of stenting followed by elucidating of hemodynamic changes in the vicinity of stents, which may follow the management of clinical amelioration of interventional treatment with aortic stenting.**

*Clinical Relevance*— **This study represents a modelling approach of the dissected aorta for endovascular intervention using stenting followed by the examination of false lumen volumetric changes resulting in the deterioration of pressure increase in diseased lesions.**

## I. Introduction

Risk of aortic dissection increases according to the ageing, and the dissection is still one of the common aortic diseases in the super-ageing society. For the treatment of aortic dissection, surgical or endovascular interventional approaches are performed by using vascular prostheses, such as stent grafts or vascular stents. Vascular replacement needs large incisions and highly invasive procedure. Although the conventional endovascular approaches with stent-grafts are performed less invasively, there is a limitation of installation at the branching sites.[1-5] The purpose of this study was to examine an aortic bare-metal stent which was capable of installing to the aortic dissected lesion for biomedical hemodynamics point of view.

Modeling approaches specific to endovascular interventional therapeutics for aortic dissection have been reported. [1, 7, 8, 11] In this study, we aimed to examine the effects of aortic stent installed at the dissected lesion of the aorta based on the measurement of natural dissected structural imaging as well as the hemodynamic changes.

Firstly, we created a goat model of descending thoracic aortic dissection, and we examined the changes in hemodynamics of dissected lesions and the amelioration by endovascular stent intervention. Secondly, we made several types of 3-D stereolithographic dissected aortic models with silicone rubber membrane between the false and the true lumens. Then, the changes in hemodynamic characteristics in the dissection model were examined in the pulsatile flow conditions in a mock circulatory system.

## II. Methods

All animals used in this study were treated in accordance with the Declaration of Helsinki and the Guiding Principles in the Care and Use of Animals. The experimental protocol for animal care was also approved by the Animal Care Committee of Tohoku University.

### *A. Methods Used to Create Aortic Dissection and Measurement of Hemodynamic Characteristics*

The experimental model of aortic dissection was created using an adult healthy goat weighing 52kg. Under the general anesthesia, we exposed the descending thoracic aorta via a left lateral thoracotomy incision. The tunica media of descending aorta was bluntly separated by using a 10-mm width spatula to create a dissection, and the entry or reentry incision was made in the intima (Figure 1).

We measured pressure and flow waveforms at the aortic root by using a fluid-filled pressure transducer (DTXplus, BD, USA) and a cuff-type ultrasound flow probe (PAU16, Transonic Systems, USA). Hemodynamic data were recorded by a digital recorder (LX110, Teac, Japan) at the sampling frequency of 1 kHz. For the comparison of hemodynamic

*Research supported by the Cooperative Research Project Program of Joint Usage/Research Center at the Institute of Development, Aging and Cancer, Tohoku University, and Grants-in-Aid for Scientific Research (KAKENHI), the Joint Research Program of Joint Usage/Research Center at the Institute of Development, Aging and Cancer, Tohoku University.

Y. Shiraishi and T. Yambe, A. Yamada are with Pre-Clinical Research Center, the Institute of Development, Aging and Cancer, Tohoku University, Sendai, Miyagi 980-8575 Japan (corresponding author to provide phone: +81 22 717 8517; fax: +81 22 717 8518; e-mail: shiraishi@tohoku.ac.jp).

Ryosuke Morita is with the Graduate School of Biomedical Engineering, Tohoku University, Sendai 980-8575, Japan.

A. J. Narracott is with the Department of Infection, Immunity & Cardiovascular Disease, University of Sheffield, Sheffield S10 2RX, UK (e-mail: a.j.narracott@sheffield.ac.uk).

Y. Qian is with the Faculty of Medicine and Health Sciences, Macquarie University, NSW 2109, Australia (e-mail: yi.qian@mq.edu.au).

K. Hanzawa is with the Department of Advanced Treatment and Prevention for Vascular Disease and Embolism, Niigata University Graduate School of Medicine and Dental Sciences, Niigata, Niigata, Japan.

changes in the systemic circulation, we calculated input impedance at the ascending aorta under the pre and post-condition of the dissecting procedure.

### *B. Modeling of 3-D Structure in Dissected Aorta*

We obtained the series of cross-sectional ultrasound images along the descending aortic longitudinal axis by an ultrasound echocardiogram diagnosis device (LogiQ, GE Healthcare, Japan). Each cross-sectional image was recorded synchronously to the electrocardiogram at 1mm intervals. We used a fixation arm for the echo probe with a linear guide placed in parallel with the descending aortic longitudinal axis. Then we reconstructed the 3-D images by the extraction of the outlines of the false and the true lumens. After the measurement and reconstruction of the dissected aorta, we made 3-D stereolithographic dissected aortic models with silicone rubber membrane between the false and the true lumens (Figure 2). From the synchronous sequences of the electrocardiogram, end-systole, and end-diastole shapes of the dissection portion were reproduced (Figure 2B). Based on the 3-D rigid models, the resin-made dissected descending aorta model was fabricated (Figure 2C). The false lumen lid was separately fabricated from the true lumen cavity, the proximal or the distal aortic flow channel. The silicone rubber membrane was sandwiched by the true lumen flow channel and the false lumen lid.

### *C. Measurement of Pressure Changes in the False Lumen of the Dissected Model in a Pulsatile Mock Circulatory System*

We used a mock circulatory system to simulate the pre- and post-installation of stents in the dissected lesion models. The mock circulatory system was composed of a) a pulse duplicator, b) a proximal and a distal compliance chambers, and c) an overflow tank to reproduce the afterload (Figure 3). The pulse duplication system was driven by a linear actuator (PWA6H010, Oriental Motor, Japan) with a microcomputer, which was to represent the natural flow velocity changes obtained at the goat ascending aortic flow waveforms. The dissection model was connected to the mock system. We measured the wall pressure waveform at the dissected false lumen from the entry to the reentry portions at 1cm intervals. Flow waveforms were obtained at the inflow and the outflow portions of the dissection models by electromagnetic flowmeters (FF20, Nihon Koden, Japan). Pressure and flow waveforms were recorded simultaneously to a recorder (PowerLab 8/35, ADInstruments, Australia) at the sampling frequency of 1 kHz.

## III. RESULTS

### *A. Dissection Model in Animal Descending Aorta*

The dissection bluntly separated in the media developed distally, and the adventitia extended to a far-off beyond the media (Figures 1 and 4). The ultrasound Doppler measurement indicated the to-and-fro flow through the entry of the dissection (Figure 4B). The changes of hemodynamics were compared with the impedance calculation in the aorta before and after the dissecting procedure (Figure 5). Aortic pressure in early-systole increased in the dissected aorta. Reflected pressure waves were examined. Earlier reflection in the dissected aorta was investigated.

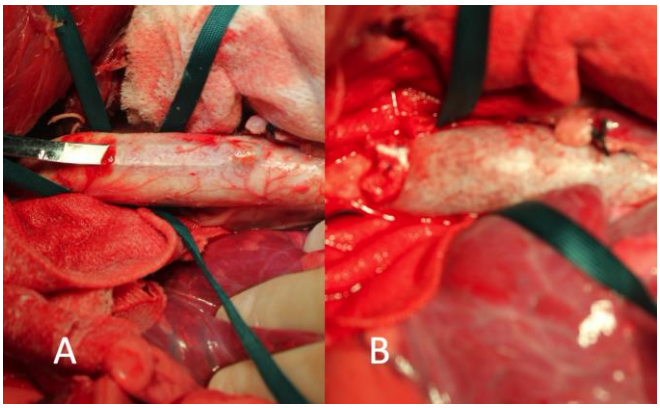


Figure 1. Dissecting procedure (A) and the dissected lesion (B) in the animal model. A spatula was bluntly inserted in the media of the descending aorta, and the entry or the reentry incisions were made. After the entry incision at the intima, the adventitia opening was surgically closed.

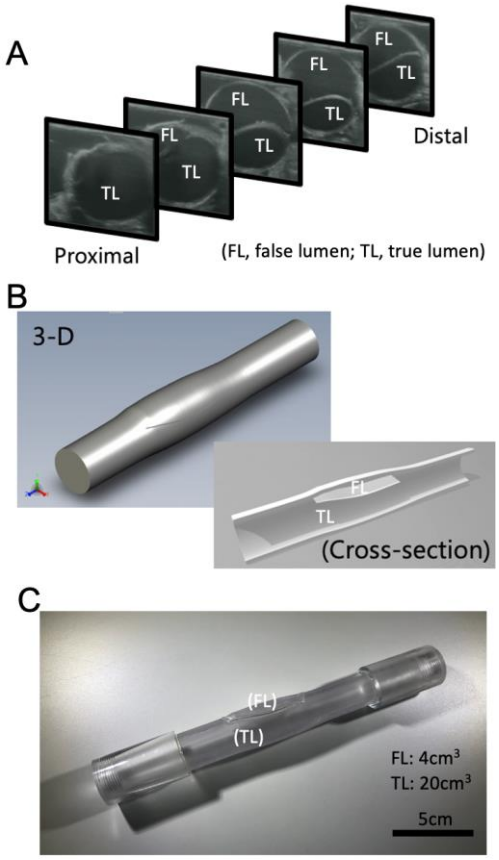


Figure 2. Modeling process from the sequential short-axis images obtained by the ultrasound imaging (A) to 3-D reconstruction (B) and the stereolithography dissection shell with the silicone rubber flap used in the study. Volumes of FL and TL were with the dissection lesion.

### *B. Stent Installation Images in the Dissection Model*

An example of the pre- and post-stenting angiography of the mock test section with the false cavity pressure ports were shown in Figure 6. After the installation of the nitinol stent, the membrane was raised and the false lumen cavity was decreased.

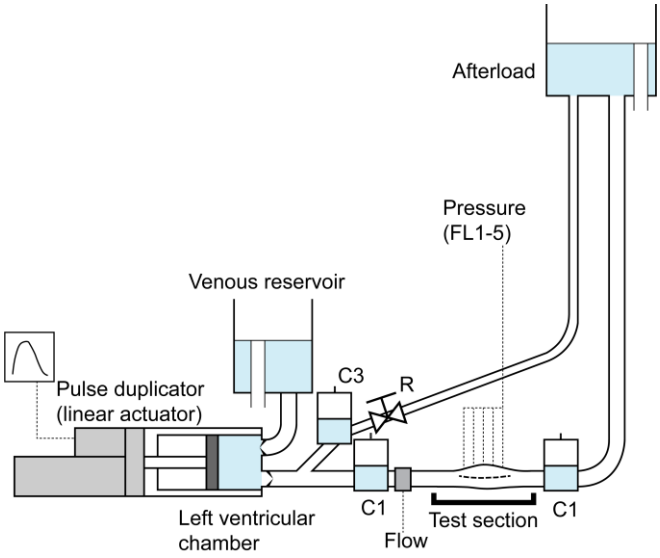


Figure 3. Schematic illustration of the mock circulatory system for the pulsatile test with the aortic dissection models. A pulse duplicator generates the aortic flow waveforms. Three compliance chambers (C1-C3), Resistance (R), and two overflow tanks as a venous reservoir and the aortic afterload were used. False lumen (FL) pressure was measured at the wall from the proximal (entry) to the distal (reentry) (FL1-5).

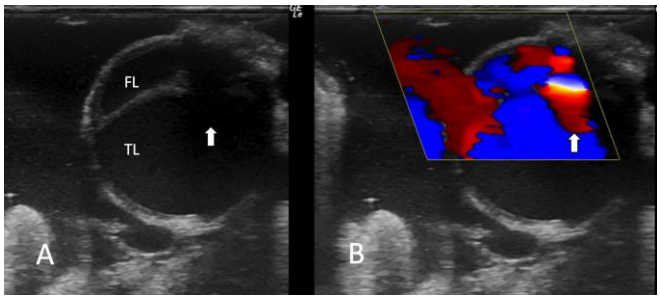


Figure 4. Short-axis ultrasound image (A) at the entry cross-section of dissection in the animal model. Each arrow shows the entry, and to-and-fro color Doppler image was obtained at the opening of the flap between the false lumen (FL) and the true lumen (TL) (B).

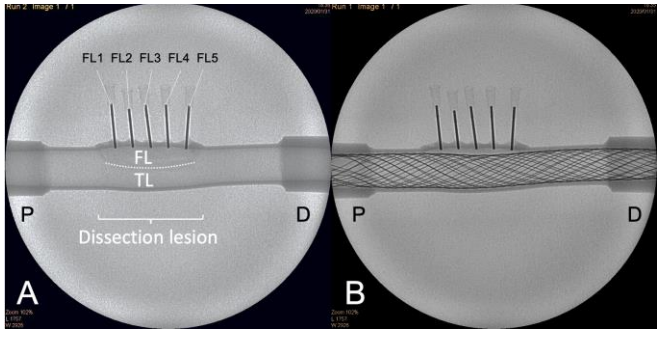


Figure 6. Comparison of the angiography obtained at the dissected aortic model (A), and the stenting model (B). Pressure ports (FL1-5) were placed to measure wall pressure in the false lumen cavity. The nitinol stent was delivered by the normal clinical intervention technique. (P, proximal; D, distal; FL, false lumen; TL, true lumen)

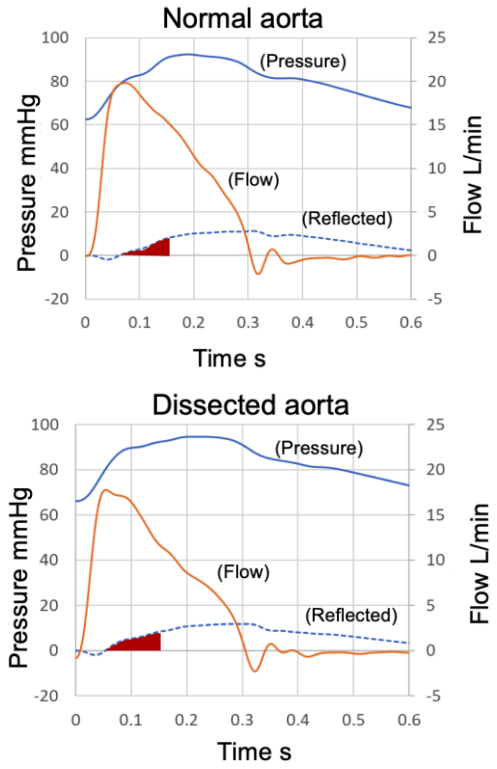


Figure 5. Comparison of hemodynamic waveforms obtained at the normal aorta before the dissecting procedure (top) and at the dissected aorta (bottom). Each reflected pressure waveform was calculated by the characteristic input impedance obtained by the pressure-flow relations. The colored area in the early-systole from 0.5 to 1.5 s indicated the difference of the wave reflection by the dissected portion of the aorta.

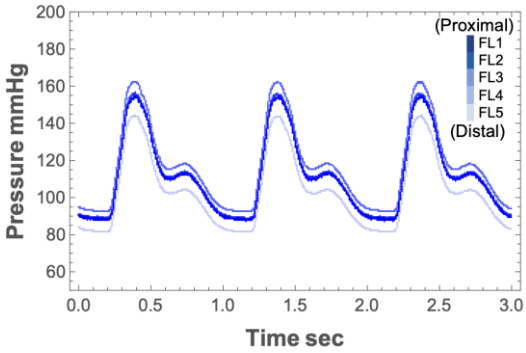


Figure 7. An example of the changes in pressure waveforms obtained from the proximal to the distal portion at the false lumen. The pressures in the vicinity of the entry or the reentry shows the lower values than the center of the dissected cavity.

### *C. Hemodynamic Changes in the Pulsatile Flow Test in the Mock Circulatory System*

Figure 7 showed an example of the changes in wall pressure waveforms obtained at the false lumen. In the central region of the false lumen cavity, the pulse pressure increased by 5-8 % compared to those values at the dissection entry in the false lumen at the constant mean flow rate of 4 L/min representing pressure increase in acute aortic dissection.

### D. *Pre- and Post-Stenting Hemodynamic Changes in the False Lumen*

Pulse pressure obtained in the false lumen was compared under the pre- or the post-stenting condition by the use of the nitinol aortic stent. There was no discernible difference in the end-diastolic pressure between the pre- or post-stenting conditions at each wall pressure port. Systolic pressure values at the center of the false lumen (FL3) were higher than the entry (FL1) or the reentry (FL5) in the pre- or the post-stenting conditions. The pulse pressure elevation through the false luminal flow channel at each wall pressure port was calculated as a ratio of the pulse pressure values at each port (FL2-5) to the pulse pressure of the entry (FL1) (Figure 8). Post-stenting pulse pressure ratio decreased from the center (FL3) to the distal locations (FL4 & 5).

## IV. Discussion

We first obtained that the hemodynamic changes in the animal dissection model by the blunt separation of media. Waveforms, as well as the impedance characteristics of the aorta, were examined to reproduce a preclinical circulatory model to evaluate the hemodynamic effects of the metal stents. We demonstrated the volumetric changes in the false lumen after the reduction of the tension between the adventitia and the intima. Our approach is to reproduce the volumetric changes in the false lumen after the extended dissection as well as to investigate the post-stenting phenomena to ameliorate the diseased lesion. The quantitative analysis is crucial in the design optimization of the novel bare stent for the purpose of remodeling of the false lumen as well as reinforcement of the true lumen to maintain the aortic flow reconstruction. The quantitative analysis is crucial in the design optimization of the novel bare stent for the purpose of remodeling of the false lumen as well as reinforcement of the true lumen to maintain the aortic flow reconstruction.

The primary result from the animal hemodynamics with dissection exhibit the friable intima, and the secondary expansion of false lumen by the intimal tear may cause a lethal aortic wall structure. Although endovascular intervention is one of the promising therapeutic methods that may be applied in elderly patients, there have been no reports considering the quantitative design strategies with the mechanical force interaction in the dissection. Reduction of the false lumen volume at the dissection may be caused by amelioration and remodeling of the lesion by the elimination of turbulent velocity flow energy consumption. Therefore, the dissection hemodynamic modeling can be useful for more sophisticated device design, even though the nonlinear properties in components might be different from deteriorating lumens.

## V. Conclusion

Animal dissection model and its 3-D model provide sufficient hemodynamic changes of interventional repair after the installation of stents developed. These modelling approaches enabled the quantitative examination of post-therapeutic effects of stenting followed by elucidating of hemodynamic changes in the vicinity of stents. Therefore, it was suggested that the biomedical engineering approach could contribute to the design of more sophisticated vascular stents as well as their biological safety evaluation.

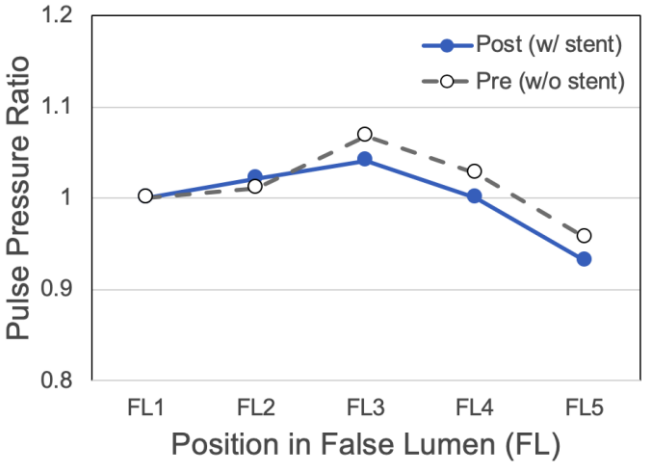


Figure 8. Comparison of the pre- and the post-stenting pulse pressure changes of wall pressure measured at the false lumen in the pulsatile flow test.

## References


[1] D. G. Mehigan, B. Fitzpatric, H. I. Browne, D. J. Bouchier-Hayes, "Is compliance mismatch the major cause of anastomotic arterial aneurysms? Analysis of 42 cases." *J. Cardiovasc Surg (Torino)*, vol. 26, no. 2, pp. 147-150, Mar-Apr., 1985.

[2] P. Marques de Marino, K. Oikonomou, E. L. Verhoeven, A. Katsargyris, "Techniques and outcomes of secondary endovascular repair for post dissection TAA/TAAA," J. Cardiovasc Surg (Torino), vol. 59, no. 6, pp. 767-774, Dec. 2018.

[3] V. K, Kotha, Z. I. Pozeg, E. J. Herget, M. C. Moon, J. J. Appoo, "Early results of the PETTICOAT technique for the management of acute Type A aortic dissection," *Aorta (Stamford)*, vol. 5, no. 4, pp. 124-128, Aug. 2017.

[4] A. C. Molinari, E. Leo, M. Ferraresi, S. A., Ferrari, A. Terzi, S. Sommaruga, G. Rossi, "Distal expanded endovascular aortic repair PETTICOAT: A modified technique to improve false lumen remodeling in acute type B aortic dissection," *Ann Vasc Surg.*, vol. 59, pp. 300-305, Aug. 2019.

[5] I. Sultan, K. Dufendach, A. Kilic, V. Bianco, D. Trivedi, A. D. Althouse, F. Thoma, F. Navid, T. G., Gleason, "Bare metal stent use in Type B aortic dissection may offer positive remodeling for the distal aorta," Ann Thorac Surg., vol. 106, no. 5, pp, 1364-1370, Nov. 2018.

[6] L. Di Tommaso, R. Giordano, E. Di Tommaso, G. Di Palo, G. Iannelli, "Treatment with transfemoral bare-metal stent of residual aortic arch dissection after surgical repair of acute type an aortic dissection," *J. Thorac Dis.*, vol. 10, no. 11, pp. 6097-6106, Nov. 2018.

[7] M. Sato, S. Kawamoto, M. Watanabe, N. Sakamoto, M. Sato, Y. Tabata, Y. Saiki, "Medial regeneration using a biodegradable felt as a scaffold preserves integrity and compliance of a canine dissected aorta," *Circulation*, vol. 126, no. 11 Suppl. 1), pp. S102-S109, Sep 2012.

[8] E. M. Faure, L. C. Canaud, P. Cathala, I. Serres, C. Marty-Ané, and P. Alric, "Human ex-vivo model of Stanford type B aortic dissection," *J. Vasc Surg.*, vol. 60, no. 3, pp. 767-775, 2014.

[9] T. Uchida, M. Sadahiro, "Thoracic endovascular aortic repair for acute aortic dissection," *Ann Vasc Dis.*, vol. 11, no. 4, pp; 464-472, Dec. 2018.

[10] A. Morishita, H. Tomioka, S. Katahira, T. Hashimoto, and K. Hanzawa, "Surgical treatment of Kommerell's diverticulum associated with a right sided aortic arch and an aberrant left subclavian artery: Endovascular or hybrid," *Ann Vasc Dis.*, vol. 12, no. 2, pp. 228-232, Jun. 2019.

[11] C. E. Korenczuk, R. Y. Dhume, K. Liao, V. H. Barocas, "Ex vivo mechanical tests and multiscale computational modeling highlight the importance of intramural shear stress in ascending thoracic aortic aneurysms," *J. Biomech Eng.*, Oct 2019.